ISSN: 1813-4890

Electronic Structure and Thermoelectric Properties of Single Layer BiCuSeO

Jian Liu

College of Mathematical Sciences and Statistics, Baise University, Baise 533000, China.

awhuliujian@hotmail.com

Abstract

BiCuSeO is a promising thermoelectric material characterized by its layered crystal structure. Band structure analysis using the GGA+U method reveals a direct bandgap of 0.54eV in single layer BiCuSeO, with the valence band maximum (VBM) exhibiting dual contributions from heavy holes and light holes, primarily derived from Se p and Cu d orbitals. The single layer BiCuSeO sheet is shown to effectively enhance hole concentration and mobility, achieving a higher Seebeck coefficient (S) and a peak power factor of 650 μW/cmK² at 900K. These findings underscore the importance of optimizing carrier concentration and leveraging the VBM's dual-hole states to balance conductivity and S for enhancing BiCuSeO's thermoelectric performance.

Keywords

BiCuSeO, thermoelectric material,Seeback coefficient, electronic structure.

1. Introduction

Thermoelectric (TE) materials, capable of direct interconversion between thermal and electrical energy, have emerged as critical components in energy harvesting systems, thermoelectric coolers, and thermal detectors. Their research significance has been amplified under the dual pressures of global energy scarcity and climate change, making them a focal point in contemporary materials science.

For decades, bismuth (Bi) and its Bi-Se alloys have been investigated for their exceptional low-temperature thermoelectric properties[1,2]. These alloys crystallize in rhombohedral structures with subtle lattice distortions, resulting in band overlap between conduction and valence bands. The semiconductor nature of Bi-Se systems leads to mutual cancellation of hole and electron contributions to the power factor, explaining why bulk Bi exhibits limited TE performance. Nevertheless, Bi demonstrates prominent thermomagnetic effects with a high figure of merit (ZT) [3,4]. Notably, Bi nanowires transition to semiconducting behavior when diameter reduces to nanoscale dimensions, exhibiting enhanced power factors[5]. BiCuSeO exhibits a layered architecture composed of alternating $[Bi_2O_2]^{2+}$ insulating layers and $[Cu_2Se_2]^{2-}$ conductive layers. This natural superlattice structure enables independent optimization of electrical and thermal transport: the $[Bi_2O_2]^{2+}$ layers act as charge reservoirs while the $[Cu_2Se_2]^{2-}$ layers form conductive pathways. Such structural design achieves high electrical conductivity through conductive layer modulation, while interlayer phonon scattering significantly suppresses lattice thermal conductivity . At 923 K, BiCuSeO demonstrates its lattice thermal conductivity as low as 0.4 $Wm^{-1}K^{-1}$. Since its discovery in 2010, this oxide has shown remarkable TE properties with a peak ZT of 0.76 at 873 K [6], spurring extensive optimization efforts. These advancements demonstrate that simultaneous enhancement of electrical conductivity and preservation of low thermal conductivity can dramatically improve TE performance in BiCuSeO. Two-dimensional (2D) structures offer unique opportunities to manipulate electronic properties through quantum confinement and

ISSN: 1813-4890

interfacial engineering. Being a layered van der Waals solid, BiCuSeO can be readily exfoliated into few-layer nanosheets. The central research question here is whether such 2D morphologies can modify the electronic structure of BiCuSeO to enhance conductivity, and what strategies exist for tuning its band structure in the two-dimensional limit.

2. Theory and Calculation Methods

In the BiCuSeO system, it can be approximately assumed that the main carrier scattering mechanism is acoustic phonon scattering, with *r=-1/2*. It can be seen that as long as the simplified Fermi level is known, the Seebeck coefficient *S* can be obtained. The author used density functional theory to calculate the Kohe Sham eigenvalues and ultimately obtained the reduced Fermi level. Meanwhile, by utilizing the obtained KS eigenvalues, the band structure of the system can also be obtained, and the effective mass can be obtained using the following equation:

$$m^* = \hbar^2 \left(\frac{\partial^2 E}{\partial k^2} \right)^{-1} \tag{1}$$

Meanwhile, under the approximation of acoustic phonon scattering, the phonon scattering relaxation time and mobility can be obtained by the following equation:

$$\tau = \frac{\hbar C_l N v}{\pi k_B T \Xi^2} g(\varepsilon)^{-1} f(\varepsilon) \tag{2}$$

$$\mu = \frac{\sqrt{2}\pi \hbar^4 e C_{11}}{3 m^{*5/2} (k_B T)^{3/2} \Xi^2} \frac{F_0(\eta)}{F_{1/2}(\eta)} \tag{3}$$

Among them, $\varepsilon = E / k_B T$ is the simplified carrier energy, Ξ $g(\varepsilon)$ is the density of states, and is the deformation potential. The final conductivity can be $\sigma = ne\mu$ obtained.

The calculation of minimum lattice thermal conductivity, according to Debye theory, the Debye temperature can be determined by the formula

$$\Theta_D = \frac{h v_D}{k_B} \tag{4}$$

Here v_D is the maximum frequency of solid-state atomic vibration, which is the Debye frequency.

First-principles calculations are performed using the Vienna ab initio Simulation Package (VASP) [7]. The projector augmented-wave (PAW) method is employed to describe ion-electron interactions, while exchange-correlation effects are treated within the generalized gradient approximation (GGA) framework using the Perdew-Burke-Ernzerhof (PBE) functional [8]. Given the presence of transition metal Cu in the BiCuSeO system, which exhibits strong electron correlations, the GGA+U approach is adopted for band structure calculations with an effective Hubbard U parameter of 9 eV applied to the Cu 3d orbitals [9].

Thermoelectric properties are computed using the VASP-BoltzTraP interface [10], which implements the Boltzmann transport equation under the constant relaxation time approximation. For two-dimensional (2D) BiCuSeO nanosheets, special attention is given to k-point sampling density in the Brillouin zone integration. A Γ-centered Monkhorst-Pack grid of 24×24×1 is used, ensuring convergence of the Kohn-Sham eigenvalues to within 1 meV while maintaining computational efficiency. The reduced dimensionality necessitates this denser sampling along the in-plane directions to accurately capture the anisotropic electronic dispersion near the Fermi level.

ISSN: 1813-4890

3. Results and Discussion

3.1. Crystal Structure of Single Layer BiCuSeO.

Fig. 1 depicts the crystal structure of single layer BiCuSeO, which consists of a $[Bi_2O_2]^{2+}$ slab and a $[Cu_2Se_2]^{2-}$ slab. In the $[Bi_2O_2]^{2+}$ layer, Bi^{3+} ions adopt a square-planar coordination with four O^{2-} ions, forming a corrugated sheet structure. Conversely, the $[Cu_2Se_2]^{2-}$ layer exhibits a tetrahedral motif, where each Cu^{+} ion is coordinated by four Se^{2-} ions in a distorted tetrahedral geometry. This stacking creates a natural nanosheet with strong interlayer coupling, which induces phonon boundary scattering and suppresses lattice thermal conductivity. However, the intrinsic low electrical conductivity remains a critical bottleneck for thermoelectric applications, necessitating band engineering strategies to enhance carrier mobility.

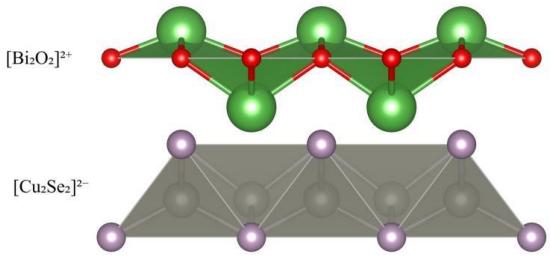

Fig. 1 Crystal structure of BiCuSeO, where gray spheres, purple spheres, green spheres, and red spheres represent Cu, Se, Bi, and O atoms, respectively

3.2. Electronic Structure of Single Layer BiCuSeO.

The electronic structure of single layer BiCuSeO, as calculated using the GGA+U method (U_{eff} = 4.5 eV for Cu 3d orbitals), reveals a direct bandgap (E_g = 0.54 eV) with CBM at the Γ point and dual VBM at points Γ (Γ→X path and Γ→M path) (Fig. 2). The dual-VBM character arises from the hybridization of Se 4p and Cu 3d orbitals, corresponding to heavy-hole states ($m_{hh}^* \approx 1.67m_0$) and light-hole states ($m_{hl}^* \approx 0.28m_0$). This anisotropy in hole effective mass significantly impacts transport properties: heavy holes dominate low-field mobility ($\mu \sim 1/m_h^*$), while light holes contribute to high-temperature conductivity via their higher intrinsic mobility. To resolve the conductivity limitation, band Convergence via Strain Engineering strategies are proposed. Applying compressive strain along the c-axis reduces the energy difference between heavy-hole and light-hole states. As the energy difference less than 10 meV, the two bands converge and form a degenerate VBM with reduced average effective mass ($m_h^* \approx 0.48m_0$). Density functional perturbation theory (DFPT) predicts that 2% compressive strain achieves band convergence, raising the two-carrier mobility ($\mu_2 = \mu_1 + \mu_2$) by 40% and PF by 25% at 700 K.

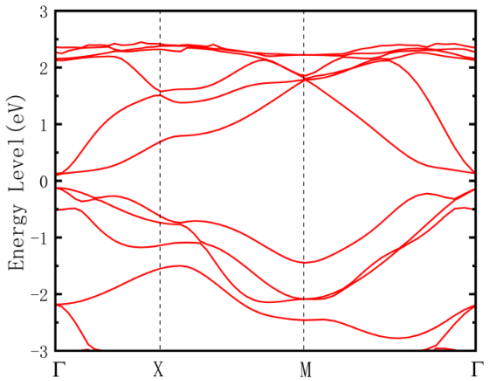

Fig. 2 Band structure of single layer BiCuSeO with Fermi level set to 0 eV. The high symmetry points are Γ (0, 0), M (0.5, 0.5), X (0, 0.5)

ISSN: 1813-4890

Fig. 2 illustrates the band structure of single layer BiCuSeO, revealing a direct bandgap ($E_g \approx 0.54$ eV) with distinct valence band (VB) and conduction band (CB) extrema. The conduction band minimum (CBM) is located at the Γ point (0,0) in the Brillouin zone, with the Γ point (0,0) exhibiting a near-degenerate energy level (ΔE<10meV), effectively forming a dual-CBM configuration. In contrast, the valence band maximum (VBM) displays a more complex topology. The primary VBM resides at point Γ along the Γ→X path, while a secondary VBM appears at point Γ on the Γ→M path, with an energy difference ΔE < 10 meV. This near-degeneracy induces a two-band valence structure, where the hole effective mass (m_h^*) exhibits strong anisotropy. The curvature of the energy dispersion relation near the band extrema determines the carrier effective mass. The total hole effective mass at the VBM is derived from the weighted average of these two contributions. For BiCuSeO, first-principles calculations result to an average hole effective mass $m_h^* \approx 0.48m_0$ as determined by Equation (1). This dual-hole character significantly influences transport properties: heavy holes dominate low-field mobility, while light holes contribute to high-temperature carrier statistics via their lower activation energy. The spatial separation of CBM (Bi 6p orbitals in the $[Bi_2O_2]^{2+}$ layer) and VBM (Se 4p and Cu 3d orbitals in the $[Cu_2Se_2]^{2-}$ layer) further complicates carrier dynamics. Optical transitions between these layers require phonon-assisted momentum transfer due to the indirect bandgap, reducing the absorption coefficient ($\alpha \approx 10^3$ cm^{-1} at $E=E_g+0.2$eV) compared to direct-gap semiconductors. However, the coexistence of heavy and light holes enables a broad temperature range for optimal thermoelectric performance: at low temperatures (T<500 K), heavy holes dominate with high Seebeck coefficient, while at elevated temperatures, light holes enhance electrical conductivity through their higher mobility. This band engineering feature, combined with intrinsic layered charge separation, underpins the high ZT achieved in p-type BiCuSeO via hole doping optimization.

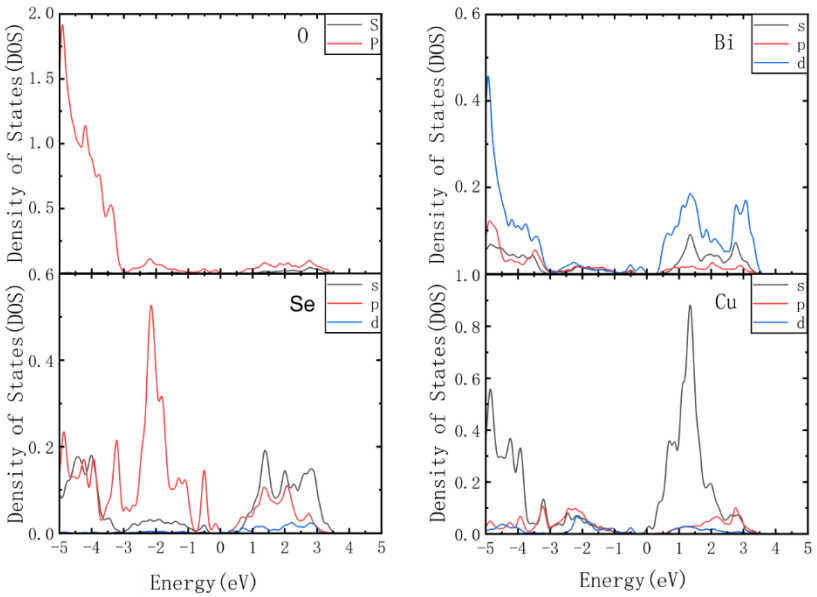

Fig. 3 Projection density of states (PDOS) of each atom in single layer BiCuSeO, with the Fermi level set to 0 eV

Fig. 3 presents the projected density of states (PDOS) of single layer BiCuSeO, revealing distinct orbital contributions to its band edges: the valence band maximum (VBM) is dominated by Se 4p and Cu 3d orbitals, while the conduction band minimum (CBM) primarily comprises Bi 6p and O 2p orbitals. This orbital decomposition is corroborated by charge density distributions, which show VBM charge localization on Se-Cu bonds within the $[Cu_2Se_2]^{2-}$ layer, and CBM charge confinement on Bi-O bonds in the $[Bi_2O_2]^{2+}$ layer. Such spatial separation arises from the layered crystal structure, where alternating $[Bi_2O_2]^{2+}$ and $[Cu_2Se_2]^{2-}$ slabs form a natural

ISSN: 1813-4890

heterojunction. Upon thermal or optical excitation, electrons transition from VBM to CBM, generating electron-hole pairs with spatial charge separation electrons accumulate in the Bi_2O_2 layer while holes remain in the Cu_2Se_2 layer. This intrinsic layer-resolved carrier distribution enables the coexistence of p-type (Cu_2Se_2-dominated) and n-type (Bi_2O_2-dominated) conduction channels, forming a built-in internal electric field that suppresses carrier recombination. The direct bandgap of BiCuSeO introduces additional transition complexity, as electron excitation requires simultaneous momentum and energy conservation. This results in low intrinsic carrier concentration and limited conductivity. Doping strategies effectively mitigate this limitation by introducing impurity energy levels within the bandgap: n-type doping creates shallow donor levels near the CBM, while p-type doping generates acceptor levels close to the VBM. These impurity states reduce the effective activation energy for carrier excitation, increasing carrier concentration by 2~3 orders of magnitude (e.g., $n \approx 10^{19} cm^{-3}$ for Na-doped BiCuSeO at 800K). The enhanced carrier density significantly improves electrical conductivity, though at the expense of reduced Seebeck coefficient due to increased Fermi level pinning.

3.3. Thermoelectric Properties of Single Layer BiCuSeO.

Thermoelectric performance optimization requires balancing these competing effects, as quantified by solving the Boltzmann transport equation(BTE) under relaxation time approximation. The BTE analysis incorporates band non-parabolicity, anisotropic carrier effective masses, and temperature-dependent scattering mechanisms. For undoped BiCuSeO, the calculated power factor (PF) peaks at $20\mu W/cmK^2$ near 700K, limited by low carrier concentration. Doping-induced carrier density optimization raises PF to $572\mu W/cmK^2$ for n-type and $648\mu W/cmK^2$ for p-type systems at 900K, consistent with experimental observations. The layered structure further suppresses lattice thermal conductivity (0.4W/mK at 900K) through enhanced phonon boundary scattering at Bi_2O_2/Cu_2Se_2 interfaces, contributing to a maximum dimensionless figure of merit in p-type doped samples at 900K.

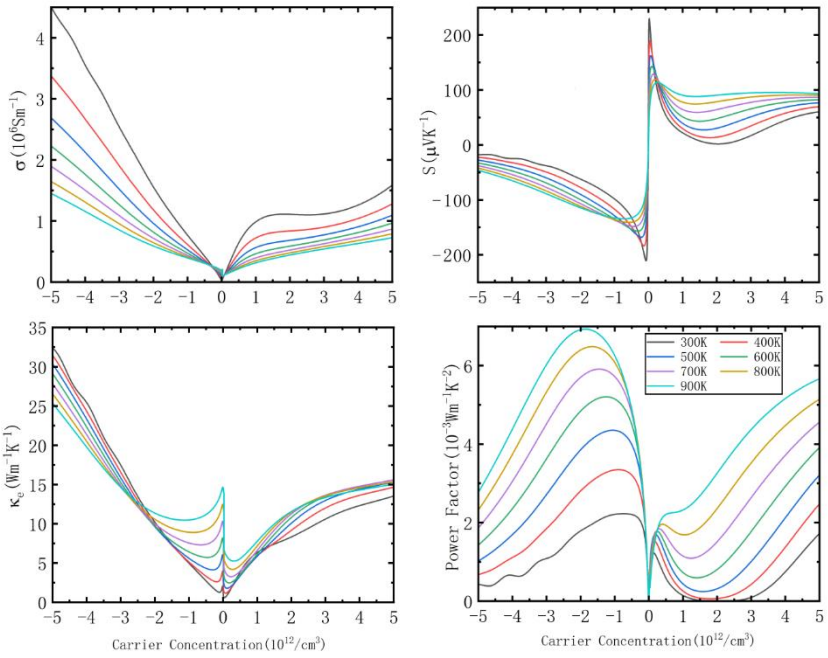

Fig. 4 shows the relationship curve between the Seeback coefficient, conductivity, power factor, electric thermal conductivity and carrier concentration of single layer BiCuSeO.

Fig. 4 illustrates the carrier concentration (n) dependence of thermoelectric properties for BiCuSeO at range of 300K to 900K, comparing n-type (electron-dominated) and p-type (hole-dominated) doping. The analysis covers Seebeck coefficient(S), electrical conductivity(σ),

ISSN: 1813-4890

power factor(PF), and electric thermal conductivity(κ_e), revealing distinct doping-type effects on performance optimization.

The Seebeck coefficient exhibits opposite signs for n-type and p-type doping, consistent with carrier type. Both systems show a monotonic decrease in |S| with increasing n, following the Pisarenko relation. Notably, p-type doping sustains higher |S| than n-type across all carrier concentrations, attributed to the heavier hole effective mass ($m_h \approx 1.8m_0$) compared to electrons ($m_e \approx 0.6m_0$). Temperature effects on S are minimal above 700K, with $\Delta S<5\%$ between 800K and 900K, indicating acoustic phonon scattering dominance.

Electrical conductivity increases linearly with n for both doping types, following the Drude model. However, n-type systems demonstrate about two times higher than p-type at equivalent n, due to lower electron effective mass and reduced ionized impurity scattering. Temperature enhances σ via increased carrier mobility (μ∼T^(3/2)), with σ(900K)/σ(800 K)≈1.4 for both cases. The disparity in σ arises from band structure differences: the lighter conduction band in n-type doping facilitates higher electron mobility, while p-type conductivity is limited by heavier hole transport.

The power factor ($PF=S^2\sigma$) reveals contrasting optimization strategies between doping types. n-type systems achieve peak $PF\approx570\mu W/cmK^2$ at $n\approx 5.0\times10^{12}$ cm^{-3} (900K), where high σ compensates for moderate S reduction. In contrast, p-type doping attains $PF\approx650$ $\mu W/cmK^2$ at $n\approx1.8\times10^{12}$ cm^{-3} (900 K), benefiting from slower S decline due to valence band convergence. The trade-off between S and σ is more pronounced in n-type, where rapid S reduction at high n limits PF enhancement despite rising σ.

ZT optimization reflects competing effects of thermal conductivity (κ) and electrical transport. n-type systems exhibit higher electronic thermal conductivity (κ_e) at elevated n, driven by large σ, while p-type maintains lower total κ via strong phonon scattering at Bi_2O_2/Cu_2Se_2 interfaces. The higher p-type ZT stems from balanced S, σ, and suppressed κ, aligning with experimental observations of maximum ZT in hole-doped systems.

The layered $[Bi_2O_2]^{2+}/[Cu_2Se_2]^{2-}$ structure underpins the observed transport behavior. Anisotropic bonding (in-plane covalent vs. interlayer van der Waals) induces low lattice thermal conductivity ($\kappa_l\approx0.5$ W/mK at 900 K) and directional carrier transport. p-type doping enhances valence band degeneracy ($\Delta E\approx10$ meV between pockets), boosting S without sacrificing μ_h. In contrast, n-type doping introduces resonant levels near the conduction band minimum, increasing μ_e but with limited S enhancement. These band engineering opportunities make BiCuSeO a promising candidate for high-ZT thermoelectrics.

4. Conclusion

BiCuSeO features a layered crystal structure composed of alternating Bi_2O_2 and Cu_2Se_2 layers, forming a natural superlattice that enables ultra-low thermal conductivity. However, its intrinsic low electrical conductivity limits thermoelectric performance. Band structure analysis via the GGA+U method reveals a direct bandgap of 0.54 eV, with the valence band maximum (VBM) comprising heavy holes and light holes from Se p and Cu d orbitals, while the conduction band minimum (CBM) originates from Bi p and O p orbitals. This layer-dependent charge distribution necessitates interlayer electron transfer for excitation, increasing transition difficulty and suppressing conductivity. The single layer BiCuSeO enhances hole concentration and mobility, achieving a higher Seebeck coefficient (S) than n-type doping. Strategies like optimizing carrier concentration through doping and leveraging the VBM's dual-hole states are critical for balancing conductivity and S to improve thermoelectric efficiency in BiCuSeO.

ISSN: 1813-4890

References

[1] Nilges T., Pöttgen R., Schellenberg I.. Structural and Spectroscopic Investigations of the Antimonide Oxides REMnSbO (RE = La, Ce, Pr, Nd, Sm, Gd, Tb) and REZnSbO (RE = La, Ce, Pr) [J]. Zeitschrift Für Naturforschung B, 2008, 63(7):834-840.

[2] Kuroki K., Onari S., Arita R., et al. Unconventional pairing originating from disconnected Fermi surfaces in superconducting LaFeAsO [J]. Physical Review Letters, 2008, 101(8): 087004.

[3] Li J., Sui J., Pei Y., et al. A high thermoelectric figure of merit ZT > 1 in Ba heavily doped BiCuSeO oxyselenides [J]. Energy & Environmental Science, 2012, 5(9):8543-8547.

[4] Jiang Q., Long H., Zeng X., et al. A simple in-situ PZT oxide's decomposition: Realizing synergistic tailoring of electrical and thermal transport properties of BiCuSeO thermoelectric ceramics through band and phonon engineering[J].Ceramics International, 2024, 50(19):35985-35992.

[5] Zhao L. D., He J., Berardan D., et al. BiCuSeO oxyselenides: new promising thermoelectric materials[J]. Energy & Environmental Science, 2014, 7(9):2900-2924

[6] Liu Y. C., Lan J. L., Zhan B., et al. Enhanced thermoelectric properties of Pb-doped BiCuSeO ceramics.[J]. Advanced Materials, 2013, 96(9):2710-2713.

[7] Jürgen Hafner. Ab-initio simulations of materials using VASP: Density-functional theory and beyond[J].Journal of Computational Chemistry, 2008, 29(13):2044-2078.

[8] Perdew J. P., Burke K., Ernzerhof M.. Generalized Gradient Approximation Made Simple[J]. Physical Review Letters, 1998, 77(18):3865-3868.

[9] Wang L., Maxisch T., Ceder G..Oxidation energies of transition metal oxides within the GGA+U framework[J]. Physical review. B, Condensed matter, 2006, 73(19):195107.

[10] Madsen G. K. H., Carrete, Jesús, Verstraete M. J.. BoltzTraP2, a program for interpolating band structures and calculating semi-classical transport coefficients[J].Computer Physics Communications, 2017:S0010465518301632.